Strain dependent magnetic, electronic, and optical properties of CrI_3/VI_3 heterostructure: A first principles study

Supplementary Information

Fazle Subhan[1], Luqman Ali[2], Nasir Shehzad[3], Yanguang Zhou[*,4] Zhenzhen Qin[*,5] and Guangzhao Qin[*,1,6,7]

1. *State Key Laboratory of Advanced Design and Manufacturing for Vehicle Body, College of Mechanical and Vehicle Engineering, Hunan University, Changsha 410082, P. R. China*
2. *Department of Pharmacology, University of Virginia, 22903, Charlottesville, VA, USA*
3. *Hunan Provincial Key Laboratory of High-Energy Scale Physics and Applications, School of Physics and Electronics, Hunan University, Changsha 410082, PR China*
4. *Department of Mechanical and Aerospace Engineering, The Hong Kong University of Science and Technology, Clear Water Bay, Kowloon, Hong Kong SAR*
5. *International Laboratory for Quantum Functional Materials of Henan, and School of Physics and Microelectronics, Zhengzhou University, Zhengzhou 450001, P. R. China*
6. *Research Institute of Hunan University in Chongqing, Chongqing 401133, China*
7. *Greater Bay Area Institute for Innovation, Hunan University, Guangzhou 511300, Guangdong Province, China*

Correspondence: maeygzhou@ust.hk (Y. Z), qzz@zzu.edu.cn (Z. Q), gzqin@hnu.edu.cn (G. Q);

Interestingly, the projected band structure for the CrI_3/VI_3 heterostructure shows that the upper layer (VI_3) originates the conduction band minimum (CBM), while the lower layer (CrI_3) originates the valence band maximum (VBM) respectively. This property of a heterostructure results in a type-II band alignment.

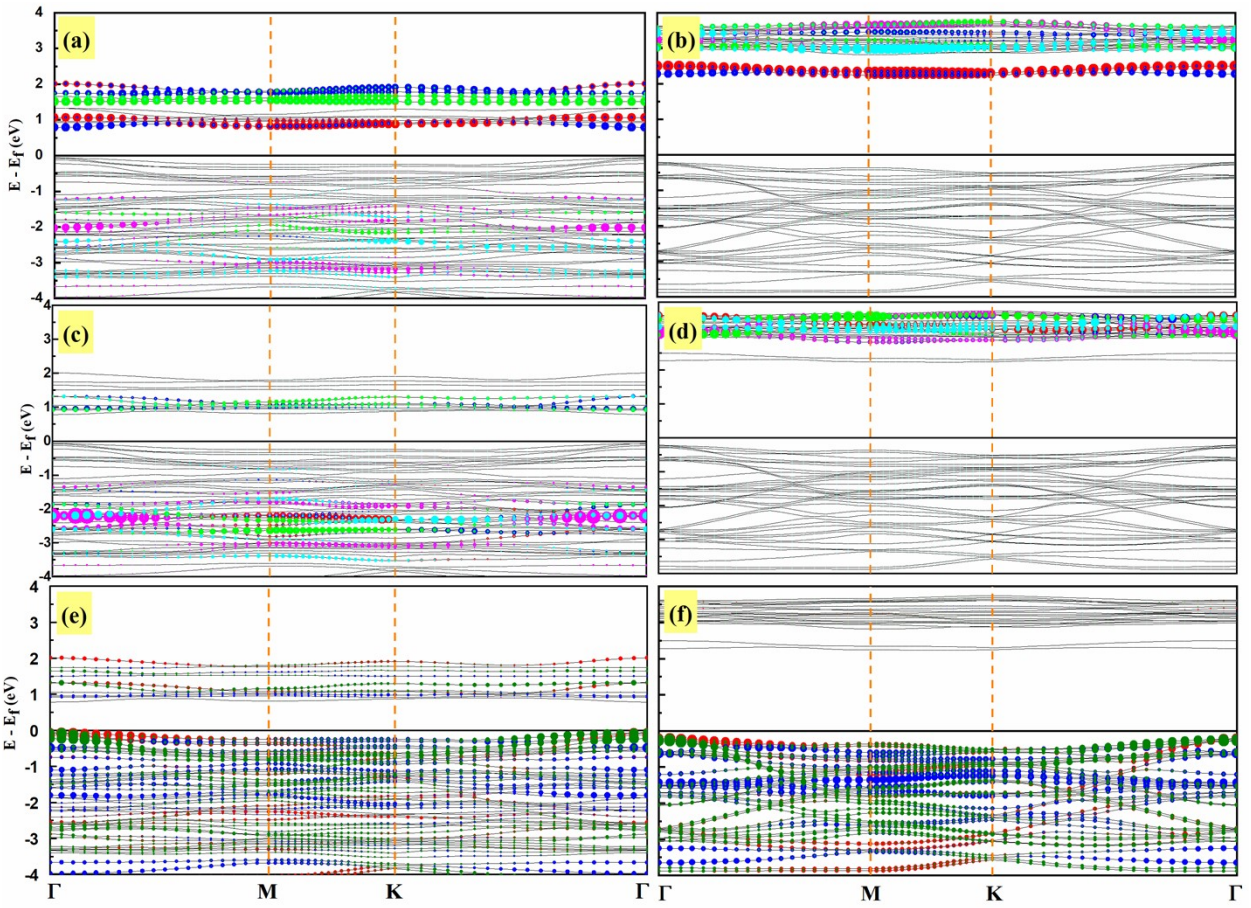

Figure SI-1 (1%T): Projected band structures of CrI_3/VI_3 heterostructure of (a-b) V, (c-d) Cr and (d-e) I atoms respectively. The first column is for majority spin while the second column shows the minority spin of the CrI_3/VI_3 heterostructure respectively.

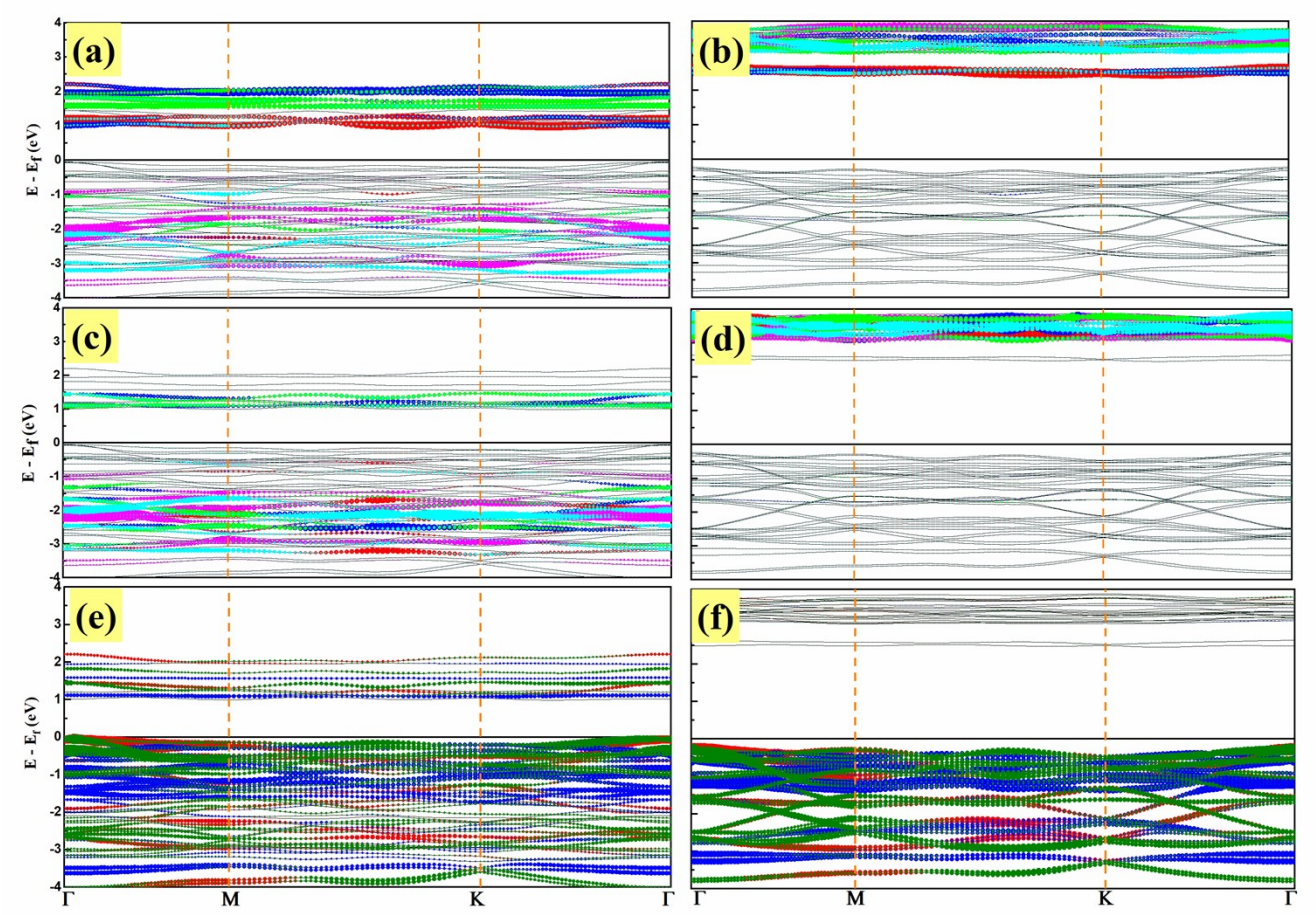

Figure SI-2(4%T): Projected band structures of CrI_3/VI_3 heterostructure of (a-b) V, (c-d) Cr and (d-e) I atoms respectively. The first column is for majority spin while the second column shows the minority spin of the CrI_3/VI_3 heterostructure respectively.

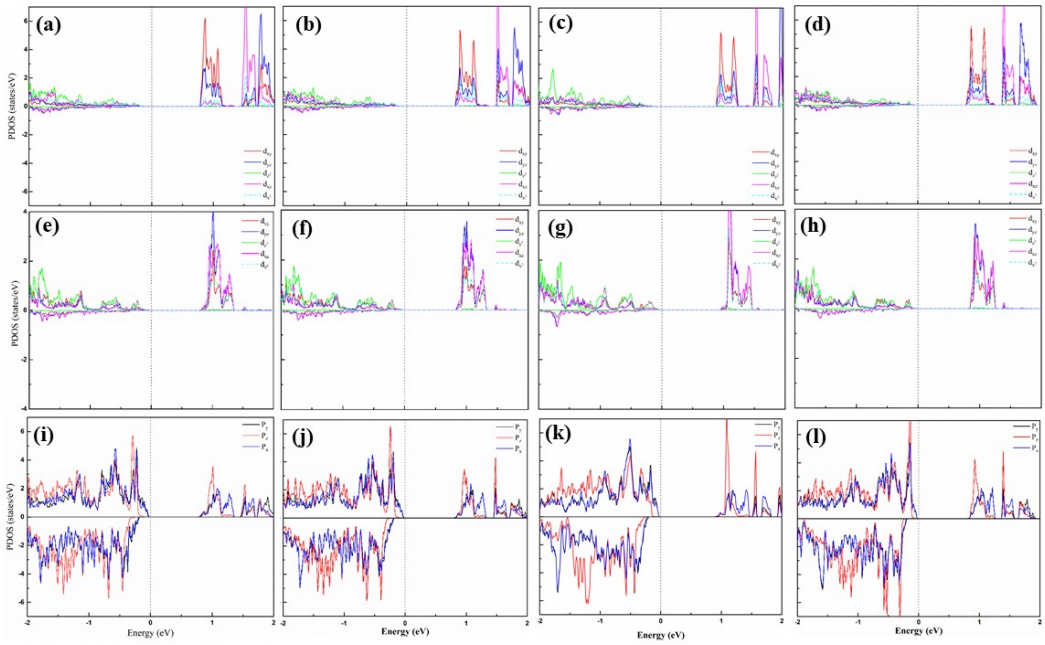

Figure ESI-3: Partial density of states of VI_3/CrI_3 heterostructure at 1 to 4 % biaxial tensile strain. The upper, middle and lower panels are respectively for V, Cr and I atoms respectively.

The first panel is for V d-orbitals and second is for Cr d-orbitals while the third panel is for I p orbitals respectively at 1 to 4% biaxial tensile strain. Like the electronic band structure, the pdos also confirm the type-II band alignment with a semiconductor nature. The PDOS is consistent with the DOS and band structure as given in the main manuscript.

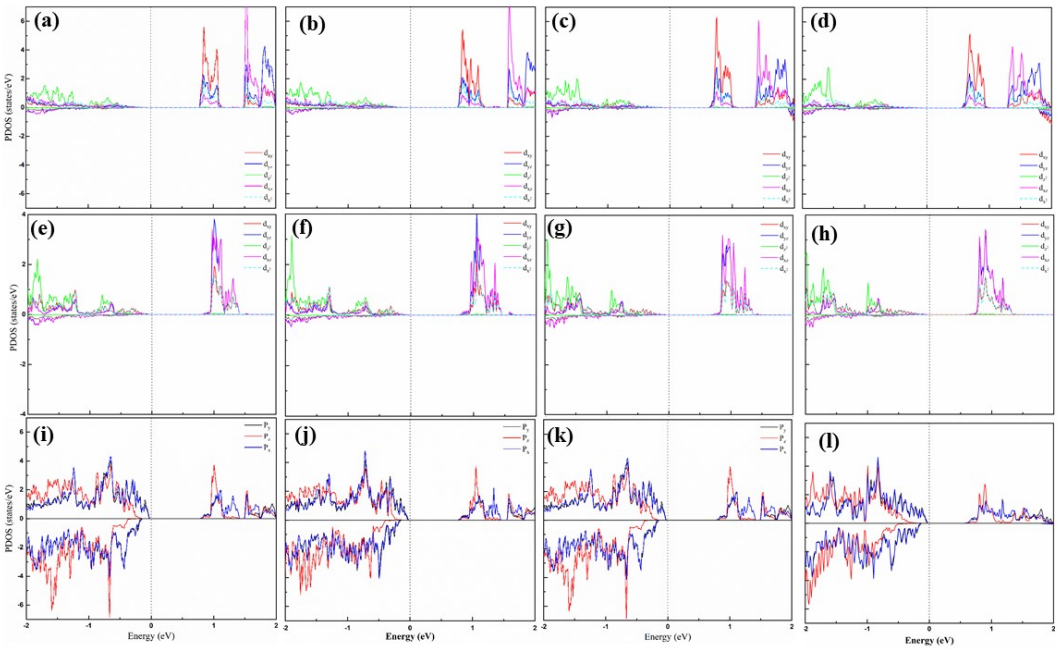

Figure ESI-4: Partial density of states of VI_3/CrI_3 heterostructure at 1 to 4 % biaxial compressive strain. The upper, middle and lower panels are respectively for V, Cr and I atoms respectively.

The first panel is for V d-orbitals and second is for Cr d-orbitals while the third panel is for I p orbitals respectively at 1 to 4% biaxial compressive strain. Similar to the electronic band structure, the pdos also confirm the type-II band alignment with a semiconductor nature. The PDOS is consistent with the DOS and band structure as given in the main manuscript.

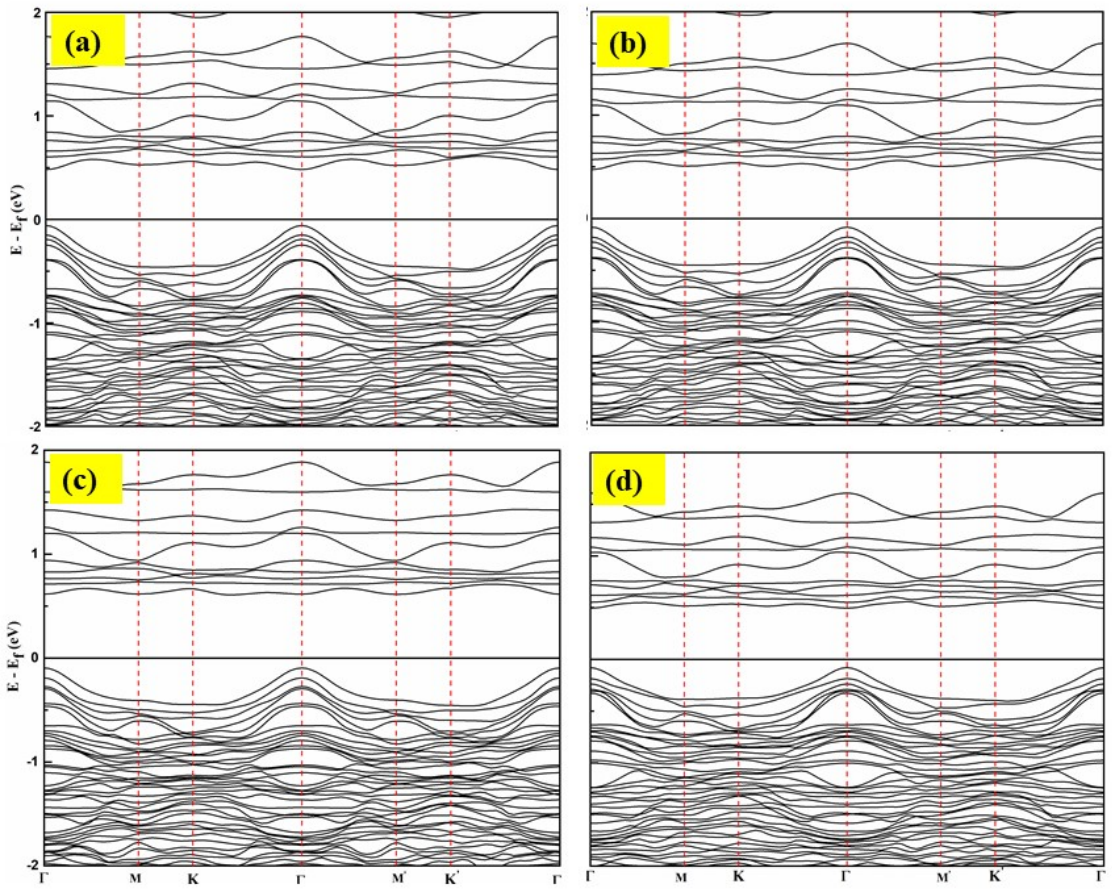

Figure SI-3: Electronic band structures of CrI_3/VI_3 heterostructure from 1 to 4% (a-d) biaxial tensile strain respectively using GGA+U with spin orbit interaction (SOC).

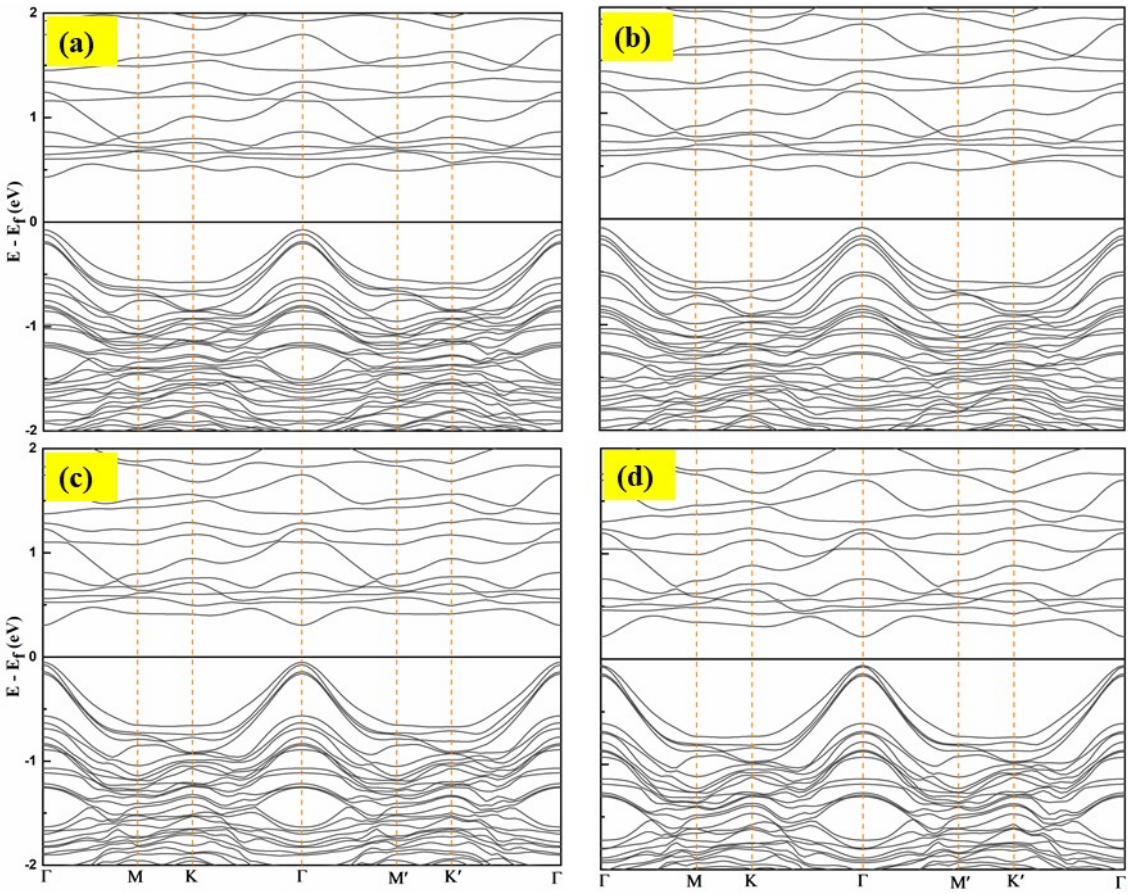

Figure SI-4: Electronic band structures of CrI_3/VI_3 heterostructure of 1 to 4% (a-d) biaxial compressive strain respectively using GGA+U with spin orbit interaction (SOC).